11TH INTERNATIONAL SCIENTIFIC CONFERENCE ON DEFENSIVE TECHNOLOGIES
OTEH 2024
Serbia, Tara, 9-11 October 2024

STRUCTURAL AND MAGNETIC PROPERTIES OF CoFeSiB AMORPHOUS WIRE GMI ELEMENT

NEBOJŠA MITROVIĆ
Faculty of Technical Sciences Čačak, University of Kragujevac, Serbia, nebojsa.mitrovic@ftn.kg.ac.rs

JELENA ORELJ
Faculty of Technical Sciences Čačak, University of Kragujevac, Serbia, jelena.orelj@ftn.kg.ac.rs

BORIVOJE NEDELJKOVIĆ
Faculty of Technical Sciences Čačak, University of Kragujevac, Serbia, borivoje.nedeljkovic@ftn.kg.ac.rs

RADOSLAV SURLA
Military Technical Institute, Belgrade, Serbia, ekorade@gmail.com

VLADIMIR PAVLOVIĆ
Faculty of Agriculture, University of Belgrade, Serbia, vlaver@agrif.bg.ac.rs

Abstract: *In this study, the amorphous soft magnetic $Co_{68.15}Fe_{4.35}Si_{12.5}B_{15}$ wires prepared by the conventional in-rotating water melt-spinning technique were investigated. The XRD pattern of the as-cast wire sample exhibits a very weak diffusive peak that reveals the amorphous structure. The DTA thermogram shows one exothermic process, which results from crystallization with a peak temperature of 566 ^{O}C. The XRD pattern of the sample annealed at 700 ^{O}C shows the presence of two diffraction peaks: the first could be ascribed to the crystal phase ε-CoSi (structure of P2 order), and the second could belong to crystal phases Co_2B and ε-CoSi (P2 order).*
The giant magnetoimpedance (GMI) frequency behavior (ranging from 50 Hz to 5 MHz) was monitored as a function of an external dc magnetic field applied parallel to the wire sample. The critical frequency of about 5 kHz - 7 kHz was observed with the initial increase of MI. In the medium frequency range (which usually starts at about 1 MHz) the skin effect and the magnetization vector rotation mechanism are dominant in the process of circular magnetization (the movement of the magnetic domain walls is blocked). Therefore, the shape of dependence of the MI-ratio on the external DC magnetic field changes significantly and the appearance of a peak is recorded. The attained peak value of the impedance modulus of about 35 Ω was registered at the highest frequency of 5 MHz. The maximum GMI ratio of 334% was recorded at a frequency of 0.95 MHz (@ 7.72 kA/m).

Keywords: *Co-rich amorphous wires, in-rotating water melt spinning, ac Joule-annealing, GMI element*

1. INTRODUCTION

The magnetoimpedance (MI) effect observed in soft magnetic wires or ribbons or thin films is one of the most interesting phenomena that can be exploited for magnetic sensors and related devices [1-3]. The impedance of ferromagnetic amorphous wires is a function of a few parameters: the operating frequency f, the intensity and orientation of the external dc magnetic field H_{ex}, and the amplitude of the alternating current I_{cc} flowing through the sample, i.e. Z (H_{ex}, f, I_{cc}) [4, 5]. The MI-effect is the result of the interactions of an external dc magnetic field with magnetic domains whose structure depends on the internal stresses evolved during the rapidly quenching process of the alloy melt in-rotating water melt-spinning technique used to produce amorphous wires. In amorphous ferromagnetic wires with a negative magnetostriction coefficient (cobalt-based alloys $Co_{68.15}Fe_{4.35}Si_{12.5}B_{15}$), the domain structure consists of the internal magnetic domain, surrounded by circular domains alternately distributed along the direction of the wire [6, 7].

In order to analyze the influence of operating frequencies on the MI-effect, two frequency ranges were examined:

(a) the low-frequency range (from about 10 kHz to about 1 MHz) in which the domain wall displacement effect is dominant [8].; and

(b) the beginning of medium frequencies (from 1 MHz to 5 MHz) in which the main influences are the skin effect and the rotation of the magnetization vector as a mechanism of the circular magnetization process (the movement of the domain walls is blocked) [9].

This paper presents structural and magnetic properties of $Co_{68.15}Fe_{4.35}Si_{12.5}B_{15}$ amorphous wires, which exhibit giant magnetoimpedance effect (GMI), i.e. they have a value of a few hundred percent of a MI ratio ($\Delta Z/Z$ (%) = 100 % $\cdot$ [$|\underline{Z}(H)| - |\underline{Z}(H_{max})|$]/ $|\underline{Z}(H_{max})|$) in a relative low dc magnetic fields (with maximum value H_{max}). This enables numerous applications of GMI-

Corresponding author: N. Mitrović;
E-mail: nebojsa.mitrovic@ftn.kg.ac.rs

DOI: 10.5937/OTEH24111M

elements as: magnetic field, rotation, pressure, and current sensors, for electronic compasses, navigation/GPS, biomagnetic measurements, magnetic memories, security systems, traffic control and industrial process, cosmic research, sports equipment, ... [10, 11].

2. EXPERIMENTAL PROCEDURE

The amorphous soft magnetic $Co_{68.15}Fe_{4.35}Si_{12.5}B_{15}$ wires with diameters of 100 μm and 120 μm were prepared by conventional in-rotating water melt-spinning technique [12, 13]. The morphology of the surface of the amorphous wires was examined by optical microscopy (OM) and scanning electron microscopy (SEM). The structural investigation was performed by the XRD experiments (Philips PW 1050 diffractometer using Cu-K_{α} radiation λ = 0.154 nm).

Thermal properties were investigated by differential thermal analysis (DTA) using TA Instruments DTA SDT 2960 at a constant heating rate of 20 ^{O}C/min., in a helium atmosphere. Chemical analysis of the constituent elements of the alloy was performed by scanning electron microscopy (SEM JEOL JSM-6390 LV) equipped with EDS Oxford Instruments X-MaxN device.

The giant magnetoimpedance (GMI) frequency behavior was monitored as a function of an external dc magnetic field applied parallel to the wire sample. The impedance of the samples of amorphous wires with a length of about 17 mm was measured by the four-point method using the LCR Hi-TESTER HIOKI 3532-50, in the frequency range from 50 Hz to 5 MHz. During the experiments performed in 1-D Helmholtz coils (H_{max} = 7.72 kA/m) the constant amplitude I_{cc} of the alternating current in wire samples was fixed at 7 mA.

3. RESULTS AND DISCUSSION

Figure 1.a shows the surface of the investigated amorphous wires recorded by optical microscopy (OM). Areas of increased roughness can be observed on the surface, created during the process of rapid quenching of the melt. During the wire magnetization process, these areas appear as pinning centers on the magnetic domain walls [14], which deteriorates the magnetically soft properties of alloys (low coercivity and high permeability) [15].

SEM micrographs of amorphous wires enable to determination of the diameter of the examined samples with large precision. The image in Figure 1.b shows slight deviations from the mean value of the wire diameter of 120 μm, thus confirming the high reliability of the technology of obtaining amorphous wires by quenching the melt of metal alloys by in-rotating water melt-spinning technique.

EDS experiments confirmed the presence and homogeneous distribution of all constituent elements in the alloy (see Figure 1.c). The DTA thermogram of the as-cast wire presented in Figure 2. shows the single exothermic process, which results from the crystallization event with a peak temperature of 566 ^{O}C.

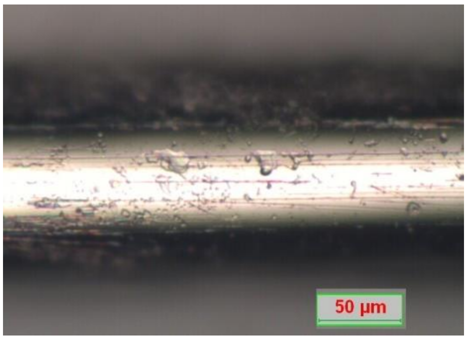

(a)

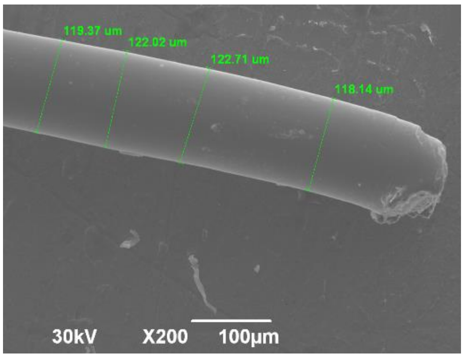

(b)

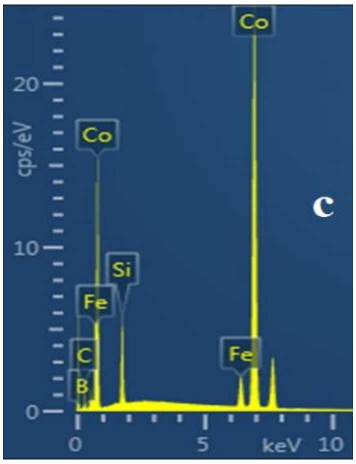

Figure 1. The surface (a), SEM micrograph (b), and elemental EDS microanalysis (c) of the $Co_{68.15}Fe_{4.35}Si_{12.5}B_{15}$ amorphous wire.

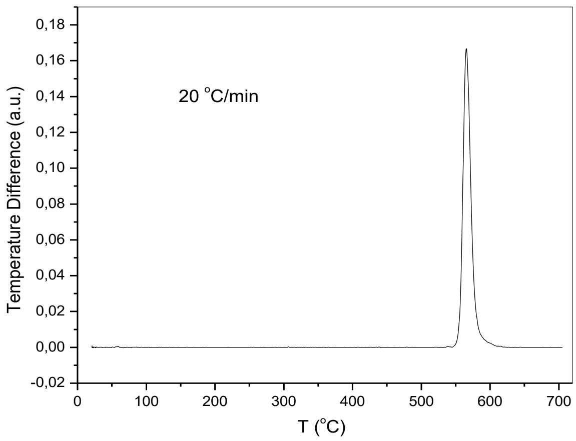

Figure 2. DTA thermogram of $Co_{68.15}Fe_{4.35}Si_{12.5}B_{15}$ as-cast 120 μm thick wire (heating rate 20 ^{O}C/min.).

The XRD pattern of the as-cast wire sample exhibits a very weak diffusive peak that reveals the amorphous structure (Figure 3.a). The XRD pattern of the sample annealed at 700 ^{O}C shows the development of two diffraction peaks: the first one that could belong to the crystal phase ε-CoSi (structure of P2 order), while the second one could be ascribed to crystal phases Co_2B and ε-CoSi (P2 order) (Figure 3.b).

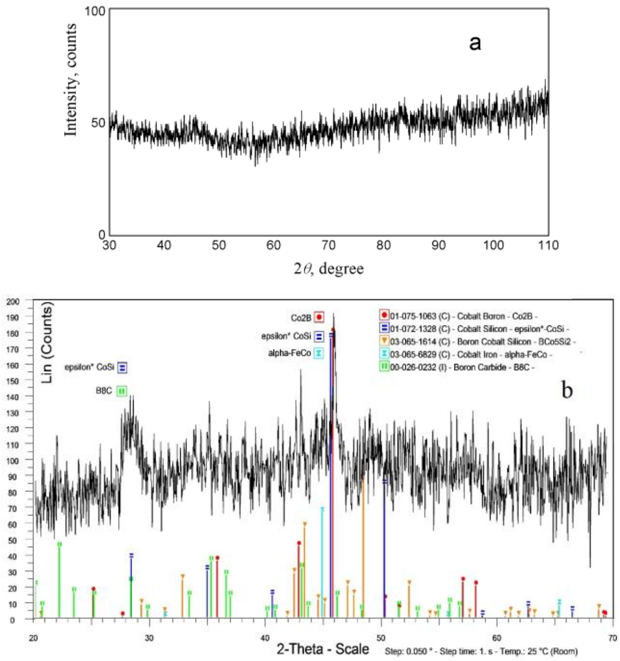

Figure 3. XRD pattern of as-cast (a) and sample annealed at 700 ^{O}C (b) of the $Co_{68.15}Fe_{4.35}Si_{12.5}B_{15}$ wire.

The as-cast wires were Joule heated with alternating current amplitude of 100 mA (@ 50 Hz) for 60 s in air, followed by slow-cooling performed on ramping down the annealing current at a rate of 5 mA/s [16]. The electrical resistivity of the 17 mm long sample remains at the constant value of 133 μΩ·cm and confirms the still amorphous and stress relief state. Figure 4. shows the frequency response of the GMI ratio in zero fields and a field H_{ex}, for different external dc magnetic fields. The critical frequency of about 5-7 kHz was observed as the point with an initial increase in the MI-effect.

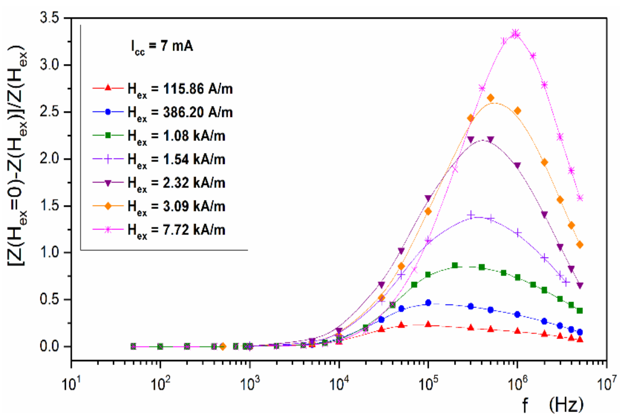

Figure 4. Frequency response of the GMI ratio in zero fields and a field H_{ex}, for different external dc magnetic fields in the range $H_{ex} \in$ [116 A/m, 7.72 kA/m].

The GMI ratio of 334% was recorded at a frequency of 950 kHz at the maximum magnetic field experiments (H_{max} = 7.72 kA/m).

Magnetic field dependence of the modulus of the impedance in the medium field range ($H_{ex} < H_{max} \approx$ 463 A/m) is given in Figure 5.

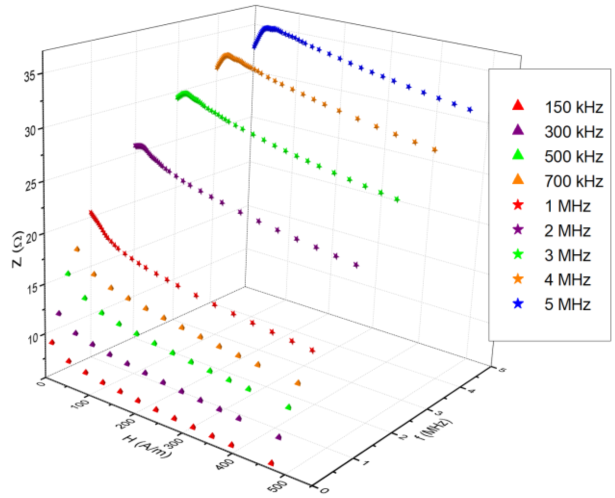

Figure 5. Magnetic field dependence of the modulus of the impedance in $Co_{68.15}Fe_{4.35}Si_{12.5}B_{15}$ wire (medium field range $H_{ex} < H_{max} \approx$ 463 A/m) and in the investigated frequency range f ∈ [150 kHz, 5 MHz].

In the range of low operating frequencies (f < 1 MHz), the magnetic permeability μ decreases with the increase of the direct magnetic field H_{ex} (at a constant frequency f and a constant amplitude of the current through the sample I_{cc}). An increase in the magnetic penetration depth δ_m (H_{ex}) results in a decrease in the impedance modulus of the wire sample. Experiments show that the curves are characterized by a constant decrease with an increase in the magnetic field, as well as a constant increase in the impedance modulus with an increase in the operating frequency. The attained peak value of the impedance modulus of about 35 Ω was registered at the highest frequency of 5 MHz. In the medium operating frequency range (which usually starts at about 1 MHz) the skin effect and the magnetization vector rotation mechanism are dominant in the process of circular magnetization (the movement of the magnetic domain walls is blocked). The shape of dependence of the MI on the external dc magnetic field changes significantly and the appearance of a peak positioned at the anisotropy field H_k for all frequencies f ≥ 2 MHz is recorded.

Figure 6. shows the MI-ratio of the tested MI-element with operating frequency as a parameter in the range f ∈ [1 MHz, 5 MHz] (at magnetic field $H_{max} \approx$ 0.463 kA/m). The highest value ΔZ/Z was registered at 1 MHz, while with a further increase in frequency, a constant decrease was recorded, as a consequence of a decrease in circular permeability. The insert in Figure 6. shows a linear increase in the magnetic anisotropy field H_k (f) with increasing frequency. Magnetic field GMI sensor operates in the region of linear increasing the impedance modulus (i.e. $H_{ex} < H_k$) [17], and therefore, the increase in the magnetic anisotropy field H_k enlarges the application region when the operating frequency increases from 2

MHz to 5 MHz.

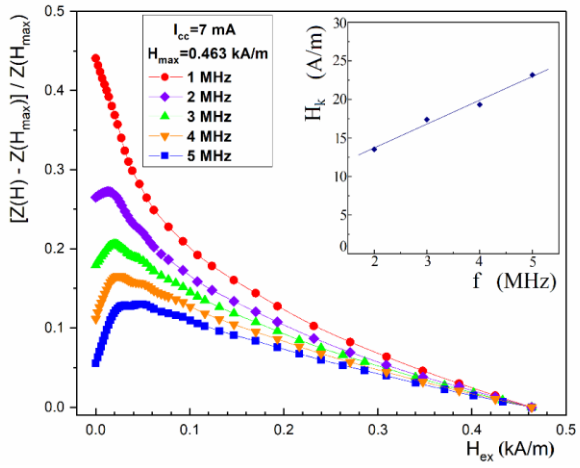

Figure 6. MI-ratio with frequency as a parameter in the range f ∈ [1 MHz, 5 MHz] ($H_{max} \approx 0.463$ kA/m).

4. CONCLUSION

The investigation of the wire GMI-element of $Co_{68.15}Fe_{4.35}Si_{12.5}B_{15}$ alloy at frequencies of the order of megahertz led to the generalized conclusion that the optimal operating frequencies are defined by the need to avoid the dominant influence of longitudinal anisotropy, i.e. the dynamics of domain magnetization inside the wire, which significantly reduces the sensitivity of the micromagnetic sensor. The attained peak value of the impedance modulus of about 35 Ω was registered at the highest frequency of 5 MHz. The dominant influence of circular magnetic anisotropy through the mechanism of rotation of the magnetization vector in the domains distributed around the circumference of the cylindrical wire leads to significant changes in the skin depth δ_m (H_{ex}, f) under the influence of a dc magnetic field and enables a significant increase in the skin depth as well as a decrease in magnetoimpedance Z. The maximum GMI ratio of 334% was recorded at a frequency of 0.95 MHz (@ 7.72 kA/m).

Acknowledgement

This research is supported in part by the Ministry of Science, Technological Development and Innovation of the Republic of Serbia, Faculty of Technical Sciences Čačak-University of Kragujevac, under Grant No. 451-03-66/2024-03/200132.

References

[1] PANINA,L.,V., MOHRI,K.: *Magneto-impedance effect in amorphous wires*, Applied Physics Letters, 65(9) (1994) 1189–91.

[2] PHAN,M.,H., PENG,H.,X.: *Giant magnetoimpedance materials: fundamentals and applications*, Progress in Materials Science, 53(2) (2008) 323–420.

[3] MITROVIĆ,N.,S., KANE,S.,N., TYAGI,P.,V., ROTH,S.: *Effect of dc-Joule-heating thermal processing on magnetoimpedance of $Fe_{72}Al_5Ga_2P_{11}C_6B_4$ amorphous alloy*, Journal of Magnetism and Magnetic Materials 320(20) (2008) e792-96.

[4] DAS,T.,K., MITRA,A., MANDAL,S.,K., ROY,R.,K., BANERJI,P., PANDA,A,.K.: *Parametric controls on giant magnetoimpedance (GMI) behaviour of CoFeSiBCr amorphous wires for prospective sensor applications*, Sensors and Actuators, A 220 (2014) 382-87.

[5] SURLA,R., VASIĆ,M., MITROVIĆ,N., RADOVIĆ,Lj., MINIĆ,D.: *Magnetic properties of $Fe_{72}Cu_1V_4Si_{15}B_8$ alloy with a composite amorphous/ nanocrystalline structure*, Journal of Magnetism and Magnetic Materials, 564(2) (2022) 170141.

[6] JIANG,S., WANG,H., ESTEVEZ,D., HUANG,Y., ZHANG,L., SHEN,H., NING,Z., QIN,F., SUN,J.: *Surface microstructural design to improve mechanical and giant magneto-impedance properties of melt-extracted CoFe-based amorphous wires*, Materials & Design, 204 (2012) 109642.

[7] LIU,J., QIN,F., CHEN,D., SHEN,H., WANG,H., XING,D., PHAN,M.,H., SUN, J.: *Combined current-modulation annealing induced enhancement of giant magnetoimpedance effect of Co-rich amorphous microwires*, Journal of Applied Physics, 115 (2014) 17A326.

[8] KNOBEL,M., VÁZQUEZ,M., KRAUS,L.: *Giant magnetoimpedance*, Handbook of Magnetic Materials, vol. 15, 1st ed. BUSCHOW,K.,H.,J. Ed., Elsevier, Amsterdam, 2003.

[9] LACHOWICZ,H.,K., GARCIA,K.,L., KUZMINSKI,M., ZHUKOV,A., VAZQUEZ,M.: *Skin-effect and circumferential permeability in micro-wires utilized in GMI-sensors*, Sensors and Actuators, A, 119(2) (2005) 384–89.

[10] MOHRI,K., YAMAMOTO,M., UCHIYAMA,T.: *Application topics of amorphous wire CMOS IC magneto-impedance micromagnetic sensors for IoT smart society*, Journal of Sensors, 2019 (2019) 8285240.

[11] KARNAUSHENKO,D., KARNAUSHENKO,D.,D., MAKAROV,D., BAUNACK,S., SCHÄFER,R., SCHMIDT,G.,O., *Self-assembled on-chip-integrated giant magneto-impedance sensorics*, Advanced Materials, 27(42) (2015) 6582-89.

[12] MASUMOTO,T., OHNAKA,I., INOUE,A., HAGIWARA,M., *Production of Pd-Cu-Si amorphous wires by melt spinning method using rotating water*, Scripta Metallurgica, 15(3) (1981) 293-96.

[13] http://www.phys-iasi.ro/en/equipment-conventional-wires-preparation, Accessed on: July. 03, 2024.

[14] BUSCHOW,K.,H.,J., DE BOER,F.,R.: *Physics of Magnetism and Magnetic Materials*, Kluwer Academic/Plenum Publishers, New York, 2003.

[15] GONZÁLEZ-LEGARRETA,L., PRIDA,V.,M., HERNANDO,B., TALAAT,A., IPATOV,M., ZHUKOVA,V., GONZÁLEZ, J., ZHUKOV,A.:

Tailoring of soft magnetic properties and high frequency giant magnetoimpedance in amorphous ribbons, High Performance Soft Magnetic Materials, ed. ZHUKOV, A. Springer Series in Materials Science, Springer Cham, 2017.

[16] ORELJ, J.,M., MITROVIĆ,N.,S., PAVLOVIĆ,V.,B.: *MI-sensor element features and estimation of penetration depth and magnetic permeability by magnetoresistance and magnetoreactance of CoFeSiB amorphous wires*, IEEE Sensors Journal, 23(13) (2023) 14017-24.

[17] NABIAS,J., ASFOUR,A., YONNET,JP.: *Temperature dependence of giant magnetoimpedance in amorphous microwires for sensor application*, IEEE Transaction on Magnetic, 53(4) (2017) 4001005.